ELSEVIER

Synthesis, characterization, and catalytic properties of $AlPO_4$-40, CoAPO-40, and ZnAPO-40

J.P. Lourenço, M.F. Ribeiro, and F. Ramôa Ribeiro
Instituto Superior Técnico, Departamento de Engenharia Química, Lisboa, Portugal

J. Rocha
Universidade de Aveiro, Departamento de Química, Aveiro, Portugal

B. Onida and E. Garrone
Università di Torino, Dipartimento di Chimica Inorganica, Chimica Fisica e Chimica dei Materiali, Torino, Italy

Z. Gabelica
Université de Haute Alsace-ENSCMu, Laboratoire des Matériaux Minéraux, Mulhouse, France

The experimental conditions leading to the synthesis of pure and highly crystalline $AlPO_4$-40, CoAPO-40, and ZnAPO-40 have been optimized. Although the preparation of these phases is favored by the presence of TMA^+ in the synthesis gel, these ions have not been found incorporated in the final AFR structures. All materials have been characterized by powder XRD, t.g./d.s.c., SEM, EDX, ^{13}C, ^{27}Al, and ^{31}P solid-state n.m.r., diffuse reflectance u.v.-vis spectroscopy, *FT* i.r., and catalytic tests using the *m*-xylene isomerization as a model reaction. This multitechnique approach provides strong evidence for the framework incorporation of cobalt and zinc. The acid sites generated by the framework insertion of cobalt and zinc are stronger than those generated by the incorporation of silicon. © Elsevier Science Inc. 1997

Keywords: $AlPO_4$-40; CoAPO-40; ZnAPO-40; synthesis; characterization; cobalt and zinc incorporation

INTRODUCTION

The synthesis of the microporous silicoaluminophosphate SAPO-40 was first carried out in 1984 by Lok et al. at the Union Carbide laboratories.[1] However, pure SAPO-40 was only obtained in 1993 by Dumont et al.[2]

SAPO-40 has a new framework topology designated as AFR by the Structure Commission of the International Zeolite Association,[3] consisting of a two-dimensional system of channels, with free diameters of 6.7 and 3.8 Å, running parallel to the *b*- and *c*-axes, respectively.[2]

Despite the important work dealing with the synthesis, characterization, and evaluation of the catalytic properties of SAPO-40 materials,[2,4–10] the conditions influencing the synthesis of related materials such as $AlPO_4$-40 and MeAPO-40 are not well known. Dumont et al.[4] found that the method leading to the synthesis of pure SAPO-40 does not allow the preparation of $AlPO_4$-40. The only phase that crystallizes in the absence of Si under these conditions is $AlPO_4$-5.

Recently, Sierra et al.[11] proposed a new method for the synthesis of $AlPO_4$-40 and MeAPO-40 (Me = Co, Zn) in which two templating agents are used, the tetrapropylammonium (TPA) ion (as hydroxide, already used in the case of SAPO-40, and/or as bromide) and tetramethylammonium (TMA) hydroxide. The use of both TPAOH and TPABr allows an appropriate adjustment of the synthesis gel pH without the introduction of other chemicals. Sierra et al.[11] have shown that it is possible to prepare AFR solids in the absence of silicon and in the presence or absence of Co or Zn. However, these syntheses afforded materials that were usually contaminated by other crystalline or amorphous phases.

In our first attempts to prepare $AlPO_4$-40 and MeAPO-40 following strictly the conditions described by Sierra et al.[11] we have obtained highly impure crystalline AFR materials. Subsequently, we have studied

Address reprint requests to Dr. Ribeiro at the Instituto Superior Tecnico, Departmento de Engenharia Quimica, Av. Rovisco Pais, 1096 Lisboa Codex, Portugal.
Received 28 March 1997

655 Avenue of the Americas, New York, NY 10010
0144-2449/97/$17.00
PII S0144-2449(97)00028-6

systematically the synthesis conditions to optimize them, and we have been successful in preparing pure and highly crystalline samples of $AlPO_4$-40 and MeAPO-40.

This paper highlights the main steps of a thorough work[12] describing the optimization of the synthesis variables leading to the preparation of pure $AlPO_4$-40, CoAPO-40, and ZnAPO-40 and their characterization by a wide range of techniques. The catalytic potential of these materials is evaluated using the isomerization of *m*-xylene as a model reaction.

EXPERIMENTAL

Synthesis

All the syntheses were carried out hydrothermally in Teflon-lined autoclaves under autogenous pressure. The reactants used were pseudoboehmite (PURAL SB, Condea) as the aluminum source, ortho-phosphoric acid (Merck, 85%) as the phosphorous source, cobalt acetate (Carlo Erba, RPE) as the cobalt source, zinc acetate (Merck, p.a.) as the zinc source, and as templating agents, tetrapropylammonium hydroxide (40% aq. sol. of TPAOH, from ALPHA), tetrapropylammonium bromide (TPABr, Merck, >99%), and tetramethylammonium hydroxide (10% aq. sol. of TMAOH from Merck).

The gels were formed by mixing two different solutions: The first solution was obtained by reacting the pseudoboehmite with diluted ortho-phosphoric acid and an aqueous solution of the metal (when used) under magnetic stirring for 4 h. The second solution was prepared by adding the TPABr and the TMAOH solution to the TPAOH solution and the remaining quantity of water. The final synthesis gel was stirred for 18 h at room temperature before introduction into the autoclaves. To study the influence of certain parameters on the synthesis, several gel compositions, crystallization times, and temperatures were tested. The stirring conditions during crystallization were also studied. After crystallization, the autoclaves were cooled down to room temperature under running water and the products were recovered by filtration or centrifugation, washed, and dried at 80–100°C overnight. For comparison, a SAPO-40 sample, synthesized according to Dumont et al.[4] and with the composition $(Si_{0.12}Al_{0.48}P_{0.40})O_2$, was used in the catalytic tests.

Characterization

The structure type and crystallinity of all the samples were checked by powder X-ray diffraction (XRD) on a Rigaku diffractometer using CuK_α radiation filtered by Ni. The crystal morphology was analyzed by scanning electron microscopy (SEM) on a Philips XL 20 microscope. The pure samples were submitted to further characterization: elemental analysis by EDX using as reference 5 as-synthesized ZnAPO and CoAPO materials of different structure and hydration state and of known molar composition; ^{31}P and ^{27}Al *MAS* n.m.r. on a Bruker MSL 400 P spectrometer operating at 9.4 T and following the conditions already described;[7] t.g./d.s.c. on a Setaram TG-DSC 111 microbalance under helium at a heating rate of 10°C/min; and *FT* i.r. analysis on a Perkin-Elmer 1760-X spectrometer using a MCT cryodetector, at a resolution of 2 cm^{-1}. The as-synthesized CoAPO-40 was also analyzed by diffuse reflectance u.v.-vis spectroscopy on a Shimadzu UV-3101PC spectrometer.

$AlPO_4$-40 was analyzed by *MAS* n.m.r. in the as-synthesized form and after calcination for 10 h under dry air at 550°C. To avoid contact with the atmospheric moisture, the calcined powder was transferred into the n.m.r. rotor under nitrogen. A ^{13}C *MAS* n.m.r. spectrum of this as-synthesized sample was also recorded.

To obtain i.r. spectra of CoAPO-40 and ZnAPO-40, the self-supported wafers were slowly calcined in vacuum up to 550°C for 5 h and then were oxidized in O_2 at the same temperature for one additional hour. After recording the i.r. spectrum, the CoAPO-40 sample was further treated under H_2 for 5 h at 500°C and a new i.r. spectrum was recorded.

Catalytic tests

Before the catalytic tests all the samples were calcined *in situ* to remove the template, by raising the temperature at 5°C/min under nitrogen flow from room temperature to 550°C and then keeping the sample at 550°C for 10 h under a flow of dry air. The temperature was then decreased to the reaction temperature under nitrogen flow. The CoAPO-40 sample was also submitted to a treatment under H_2 for 5 h at 500°C after the calcination at 550°C and a purge with nitrogen. The catalytic tests were carried out using *m*-xylene (Merck p.a.) in a fixed-bed reactor at 350°C, 1 bar, a molar ratio N_2/HC of 15 and WHSV = 17.4 h^{-1}. The reaction products were analyzed by gas chromatography using a capillary column Superox FA (Altech).

RESULTS AND DISCUSSION

Synthesis of $AlPO_4$-40

Starting from the conditions given by Sierra et al.,[11] it was not possible to reproduce the synthesis of $AlPO_4$-40. After some exploratory experiments, the following was adopted as the initial composition, from which we have started optimizing the various parameters: 0.8 Al_2O_3 : 0,8 P_2O_5 : 1.0 $(TPA)_2O$: x $(TMA)_2O$: 80 H_2O. Using a gel composition similar to that given in Ref. 11, with a TPABr/TPAOH ratio of 0.36 and x = 0.047, we only have obtained an amorphous phase after 120 h of heating at 150°C. Next, we have tried x values of 0, 0.02, and 0.046 and the TPABr/TPAOH ratio of 1.1. It was important to take into account the pH changes with the ratio TPABr/TPAOH. For example, we obtained a pH value of 6.5 for TPABr/TPAOH = 1.1 and a value of 7.5 for TPABr/TPAOH = 0.36, for x values of 0.046 and 0.047, respectively. A series of gels prepared with variable TPABr/TPAOH ratios and x values were introduced into autoclaves, both under static and stirring conditions and kept at 150°C for 120 h. The results are given in *Table 1*, and they clearly indicate that the presence of TMAOH strongly influences the final re-

Table 1 Influence of the TPABr/TPAOH and TMA/TPA ratios and of agitation conditions on the nature of the crystalline phase grown from a gel having the molar composition 0.8 Al_2O_3 : 0.8 P_2O_5 : 1.0 $(TPA)_2O$: x $(TMA)_2O$: 80 H_2O (150°C for 120 h)

TPABr/ TPAOH	TMA/TPA	Agitation	Final phase (XRD)
0.36	0.047	No	Amorphous phase
1.1	0	No	$AlPO_4$-40 + $AlPO_4$-5
1.1	0	Yes	$AlPO_4$-5
1.1	0.02	No	$AlPO_4$-40
1.1	0.02	Yes	$AlPO_4$-40
1.1	0.046	No	$AlPO_4$-40 + amorphous phase
1.1	0.046	Yes	$AlPO_4$-40 + amorphous phase

sult. A higher x-value often yields a product with incomplete crystallization, and this suggests that a large amount of TMAOH in the synthesis gel prevents the crystallization of both the AFR and AFI structures. The presence of a small amount of this compound in the gel (x = 0.02) affords the purest AFR samples. The AFR phase is also present in the final product when no TMAOH is added to the synthesis gel and when the crystallization occurs in static conditions but the samples are contaminated with the AFI phase. This result indicates that $AlPO_4$-40 can be synthesized with only the tetrapropylammonium ion (TPA) as a templating agent. When TMAOH is added to the synthesis gel, the crystallization does not seem to be influenced by stirring.

The purest $AlPO_4$-40 phase was obtained for a TPABr/TPAOH ratio of 1.1. A lower value of this parameter (which increases the pH) did not result in the crystallization of the AFR structure. This is in accord with Dumont et al.[4] who did not obtain $AlPO_4$-40 using the synthesis method developed for SAPO-40 that required only TPAOH as the source of the tetrapropylammonium template.

Using the gel composition given above, with x = 0.02 and TPABr/TPAOH = 1.1, the crystallization temperatures 130, 150, and 170°C were tested. The results show that the times to reach the maximum of crystallinity are 160 h at 130°C and 120 h at 150°C. When the gel is heated at 170°C the final product was always a mixture of AFR and AFI phases.

The above results suggest that highly pure $AlPO_4$-40 is obtained after heating for 140 h at 150°C from a gel having the following composition: 0.8 Al_2O_3 : 0,8 P_2O_5 : 1.0 $(TPA)_2O$: 0.02 $(TMA)_2O$: 80 H_2O; with TPABr/TPAOH = 1.1.

Incorporation of cobalt and zinc in the AFR structure

To incorporate cobalt in the AFR structure the first syntheses were carried out using the SAPO-40[4] method, in the presence and absence of silicon. An 8% molar composition of Co and Si in the synthesis gel was used. Under these conditions, when no silicon was added to the gel, the main product obtained was either an amorphous phase or the AFI structure. In the presence of silicon, the resulting product has the AFR structure and is identified as either CoAPSO-40 or SAPO-40. The

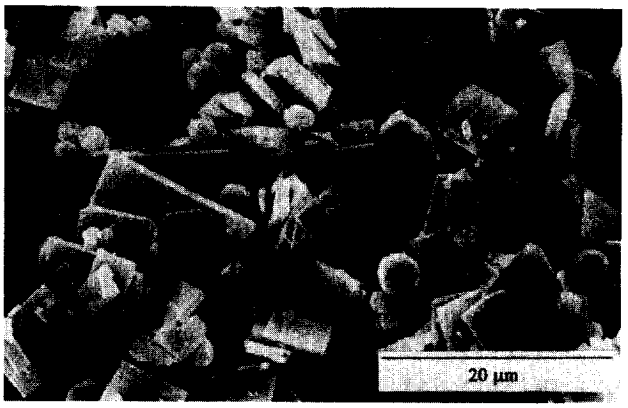

Figure 1 SEM micrograph of the final product obtained from a cobalt-loaded gel that usually crystallizes into SAPO-40.

SEM micrographs showed the presence of yet another phase with a spherical morphology (*Figure 1*). This phase did not exhibit any extra peak in the XRD pattern so far. Spot EDX analysis on selected spheres revealed a composition that was rich in cobalt but that was definitely not typical of a metallo-silicoaluminophosphate. The evidence gathered suggests that these spheres are an amorphous phase rich in cobalt. On the other hand, the color of the phase was pink, suggesting that cobalt was not tetrahedrally coordinated[13,14] in any of the AFR or amorphous Co-rich phases. Several platelet-like AFR crystals were analyzed by EDX, but no cobalt was found. Thus, this phase must be SAPO-40.

After the results reported by Sierra et al.[11] and the first results obtained in our laboratory for the synthesis of $AlPO_4$-40,[12] the following new series of conditions were tested to incorporate cobalt and zinc in the AFR structure. As already described for the synthesis of $AlPO_4$-40, several parameters were evaluated to find out the optimal conditions leading to products of high purity. A gel composition similar to that used for the synthesis of the $AlPO_4$-40 was selected: 0.8 Al_2O_3 : 0,8 P_2O_5 : 0.042 CoO : 1.0 $(TPA)_2O$: x $(TMA)_2O$: 80 H_2O; with x values adjusted to 0.0, 0.02, and 0.044 and a TPABr/TPAOH ratio fixed as 1.0. The final pH of the synthesis gel was 6.7. The crystallization occurred in static conditions for 140 h at 150°C. Other crystallization temperatures gave results similar to those obtained for the $AlPO_4$-40 synthesis. The presence of TMAOH in the synthesis gel seems to have the same effect in controlling the nature of the final product in the presence of cobalt as it has in the synthesis of $AlPO_4$-40 (*Table 2*). However, the presence of cobalt ions seems to stabilize rather easily other crystalline phases such as CoAPO-5 and CoAPO-37 (identified by XRD). In the absence of TMAOH, the resulting product was always CoAPO-5,

Table 2 Influence of the TMA/TPA ratio on the synthesis of the CoAPO-40

TMA/TPA	Final phase (XRD)
0.0	CoAPO-5
0.02	CoAPO-40
0.044	CoAPO-37

Table 3 Influence of the TPABr/TPAOH molar ratio (pH) on the synthesis of the CoAPO-40

TPABr/TPAOH	Gel pH	Final phase (XRD)
0.5	7.4	CoAPO-40 + amorphous phase
1.0	6.7	CoAPO-40
1.5	4.7	CoAPO-5
2.0	3.9	CoAPO-5

and when the value of TMAOH was close to that used for the synthesis of SAPO-37,[1] CoAPO-37 was readily obtained. All the products exhibited a good crystallinity and a deep blue color, which is a qualitative indication of the tetrahedral coordination of Co(II).

The pH of the gel is also a variable that must be controlled during the crystallization of this class of materials. Its adjustment was achieved by varying the TPABr/TPAOH ratio. A value of TMAOH/TPAOH ratio of 0.02 was selected with all the other conditions maintained at a constant. The results of this first series of syntheses are presented in *Table 3*. The value 1.0 for the TPABr/TPAOH ratio gives the best results for the synthesis of CoAPO-40. The pH of the gel, 6.7, is similar to that used in the synthesis of $AlPO_4$-40. A higher pH value results in a product with an incomplete crystallization, and a lower value results in the formation of the AFI structure. It should be noted that changing the pH by changing the TPABr/TPAOH ratio introduces different amounts of bromide ions in the synthesis gel, which may influence the purity of the final product.

The preparation of samples from gels involving a higher amount of cobalt indicated that a product with a small amount of amorphous phase can be obtained if the TPA content is reduced with respect to the amounts of Al and P. For example when a 1.3% Co molar ratio (with respect to the total amount of T-atoms) was used in the synthesis gel the composition that yielded the most crystalline CoAPO-40 was: 1.0 Al_2O_3 : 1.0 P_2O_5 : 0.042 CoO : 1.0 $(TPA)_2O$: 0.02$(TMA)_2O$: 80 H_2O; with TPABr/TPAOH = 1.0.

This study has shown that the AFR structure can be prepared in the presence of cobalt, in conditions similar to those leading to the synthesis of $AlPO_4$-40. A highly pure sample was also obtained when zinc was used instead of cobalt. Both the powder XRD pattern and Zn content determined by EDX on selected platelet-like crystals confirmed the formation of ZnAPO-40.

Characterization

Powder X-ray diffraction

Figure 2 displays the powder XRD patterns of $AlPO_4$-40, CoAPO-40, and ZnAPO-40 synthesized under the conditions described above and, for comparison, the pattern of a sample of SAPO-40. All the samples display an XRD pattern that matches that of the AFR structure. No other crystalline phase could be detected. The unit-cell parameters calculated in the orthorhombic space group (Pccn)[15] are gathered in *Table 4*. The $AlPO_4$-40 and CoAPO-40 results are similar to those reported by Sierra et al.[11] The changes that occur in the MeAPO-40

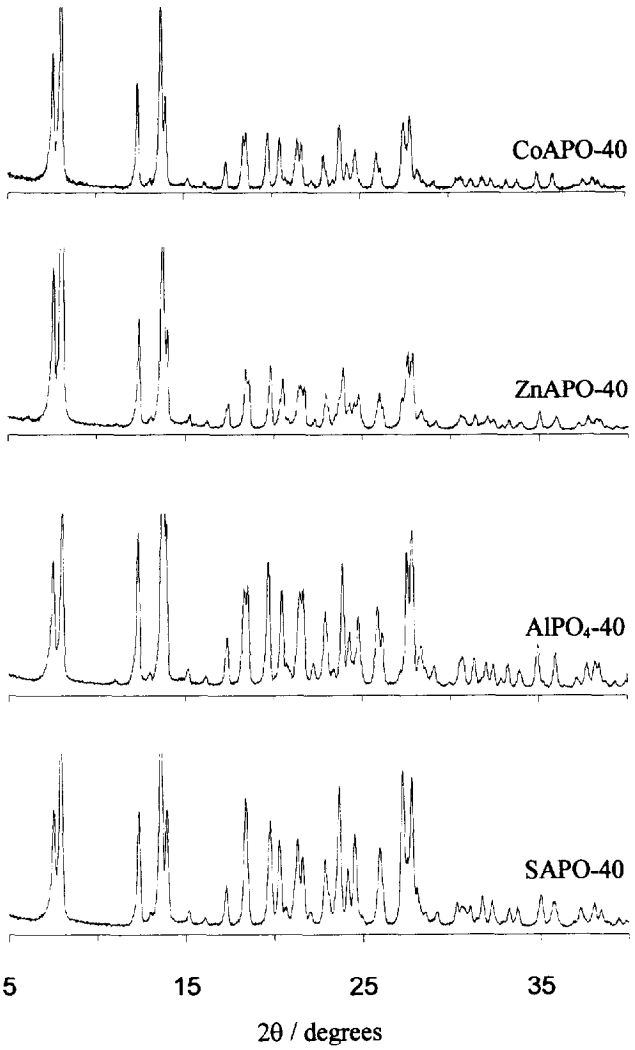

Figure 2 XRD patterns of $AlPO_4$-40, CoAPO-40, ZnAPO-40, and SAPO-40.

patterns with respect to $AlPO_4$-40 patterns are considered as an indication that, at least, some metallic ions are incorporated in the framework.[16,17] Note also that the unit-cell volume increases with respect to that of $AlPO_4$-40, which reflects the difference in the M–O lengths (Co–O > Al–O) and is thus another indication of the framework incorporation of Co.

Table 4 Unit-cell parameters of the orthorhombic AFR phases

Sample	a (±0.01 Å)	b (±0.01 Å)	c (±0.01 Å)	V (±15 Å^3)
$AlPO_4$-40	21.70	13.75	14.22	4243
$AlPO_4$-40[a]	21.72	13.75	14.22	4247
CoAPO-40	21.89	13.69	14.26	4273
CoAPO-40[a]	22.06	13.69	14.28	4313
ZnAPO-40	21.75	13.69	14.21	4231
SAPO-40[b]	21.94	13.69	14.25	4280

[a] From Ref. 11. The CoAPO-40 sample has the composition $(Co_{0.053}Al_{0.448}P_{0.499})O_2$.
[b] From Ref. 2.

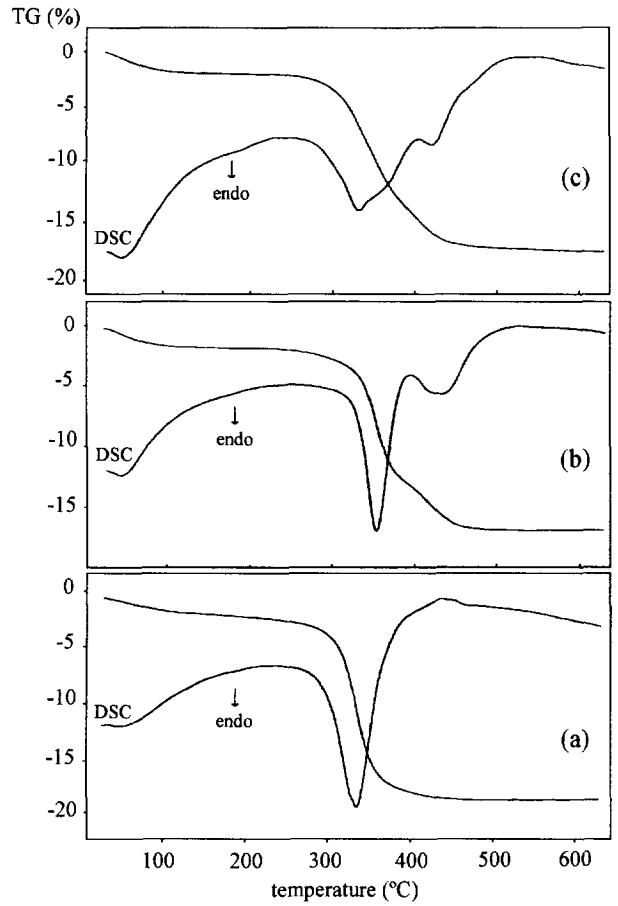

Figure 3 t.g.-d.s.c. diagrams of $AlPO_4$-40 (*a*), CoAPO-40 (*b*), and ZnAPO-40 (*c*).

Thermal analysis (t.g.-d.s.c.)

The combined t.g.-d.s.c. diagram of $AlPO_4$-40 obtained under helium flow is shown in *Figure 3a*. The endothermic peak seen in the d.s.c. curve with a maximum at ca. 340°C corresponds to the template decomposition. The weight loss at this stage corresponds to four TPA^+ ions per double unit cell, as reported by Dumont et al.[2] for SAPO-40. This result suggests that only the TPA^+ ions are entrapped within the pore structure of $AlPO_4$-40. On the other hand, the d.s.c. diagrams of CoAPO-40 and ZnAPO-40 exhibit at least two endothermic peaks also corresponding to the template decomposition (*Figure 3, b* and *c*). Again, the weight loss between 250 and 550°C indicates the presence of four TPA^+ ions per double unit cell. In contrast to the thermal behavior of $AlPO_4$-40, those of Zn- and CoAPO-40 show that the decomposition of the template occurs in successive steps, as reported for SAPO-40.[2] Such a behavior was attributed to two types of TPA species. The low-temperature loss corresponds, most probably, to the nonoxidative degradation of TPAOH, the only species present in $AlPO_4$-40. On the other hand, framework Co^{II} and Zn^{II} would generate negative charges that would interact with TPA^+ ions. These latter associations being stronger than TPAOH ionic pairs, as observed in the case of ZSM-5,[18] would decompose at a higher temperature. Although it would be inaccurate to calculate the actual metal content from the relative intensities of the two corresponding d.s.c. peaks, their simple presence may be considered as a qualitative indication of the metal incorporation.

Figure 4 SEM micrographs of $AlPO_4$-40 (*a*), CoAPO-40 (*b*), and ZnAPO-40 (*c*).

Scanning electron microscopy

The $AlPO_4$-40, CoAPO-40, and ZnAPO-40 samples are highly pure (*Figure 4*). All the products have the characteristic plate-like morphology of SAPO-40.[2] As already reported,[11] the end of the plates depends on the composition. The substituted $AlPO_4$-40 materials like CoAPO-40, ZnAPO-40, or SAPO-40 show crystals with rectangular ends, whereas the crystals of the nonsubstituted $AlPO_4$-40 show a beveled end. We have observed that the temperature of crystallization influences

Table 5 Chemical framework composition (EDX) of the as-synthesized AFR-samples

Sample	Al	P	Me
$AlPO_4$-40	50.0	50.0	
CoAPO-40	48.9	50.1	1.0
ZnAPO-40	49.2	50.0	0.8

the morphology of the $AlPO_4$-40 crystals. At 170°C the crystals have rectangular ends, whereas at 130°C the crystals show a pronounced beveled shape.

The elemental composition of the as-synthesized samples, as determined by EDX, is reported in *Table 5*. The results are in agreement with an incorporation of cobalt and zinc in the Al positions of the $AlPO_4$-40 framework.

Diffuse reflectance u.v.-vis spectroscopy

u.v.-vis spectroscopy has been widely used to probe the isomorphous substitution of cobalt in aluminophosphate-based molecular sieves. The presence of intense absorption bands near 542, 583, and 623 nm in the spectrum is characteristic of cobalt in tetrahedral coordination[13,14,19–22] and thus as an indication of isomorphous substitution. The spectrum of the as-synthesized sample of CoAPO-40 shows the characteristic profile of four-coordinated Co (*Figure 5*) and thus confirms the insertion of Co in the AFR framework.

Nuclear magnetic resonance spectroscopy

The as-synthesized samples were studied by ^{27}Al and ^{31}P *MAS* n.m.r. (*Figures 6* and *7*). In contrast to what was observed with SAPO-40, the spectra of $AlPO_4$-40 show several resonance lines that can be assigned to four-coordinated Al and P. The ^{27}Al spectrum shows four main peaks at 38.5, 37, 18, and 9.8 ppm and also two shoulders at 42 and 31 ppm. The ^{31}P n.m.r. spectrum of this material also shows several peaks in the range −15 to −30 ppm.

The incorporation of other elements in the framework, which change the strict alternation of Al and P in the tetrahedral positions, seems to change the shape of the ^{27}Al and ^{31}P n.m.r. spectra. The ^{27}Al spectra of both

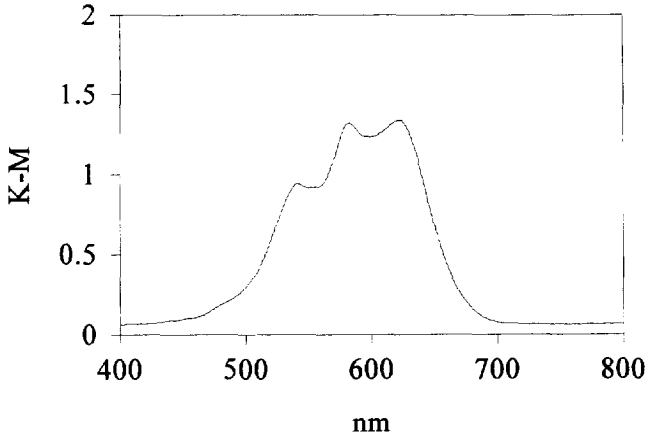

Figure 5 u.v.-vis diffuse reflectance spectrum of CoAPO-40.

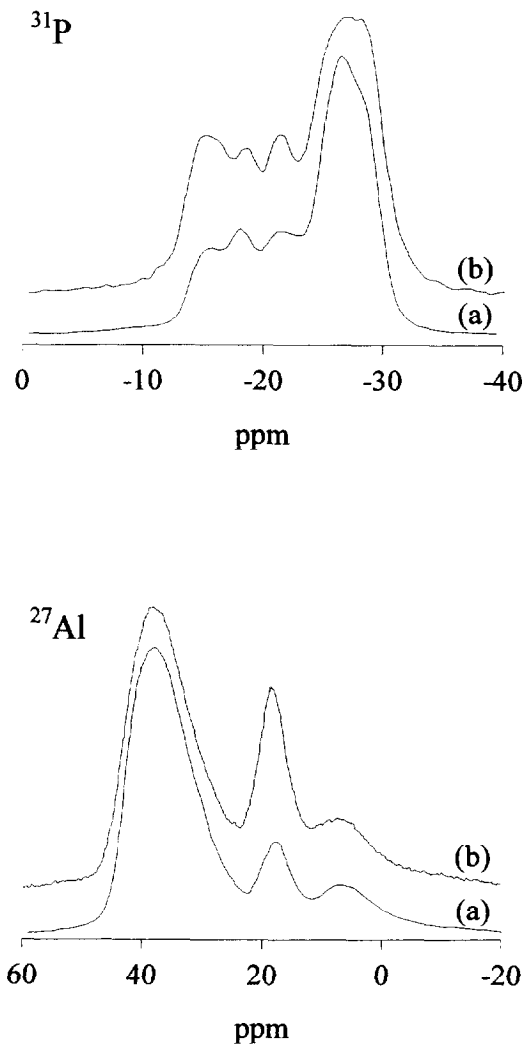

Figure 6 ^{31}P and ^{27}Al *MAS* n.m.r. spectra of as-synthesized ZnAPO-40 (*a*) and CoAPO-40 (*b*) samples.

the CoAPO-40 and ZnAPO-40 are similar to that already reported for SAPO-40.[2,7] They show an unresolved peak at 38 ppm and two peaks at 18 and 9.8 ppm. It is interesting to note that the relative intensity of the peak at 18 ppm, which has been assigned to four-coordinated aluminum interacting with the template,[2] is lower in the spectra of MeAPO-40 samples than in the spectrum $AlPO_4$-40. The spectrum of SAPO-40 shows a relatively low intensity for this peak[2,7] as well.

The resolved peaks in the ^{27}Al spectrum of the $AlPO_4$-40 sample, all of which can be assigned to four-coordinated aluminum, probably reflect the existence of several crystallographically nonequivalent positions in the structure. The introduction of different elements such as Si, Co, or Zn possibly causes local distortions and creates defect groups, which can induce broadening of the peaks. Indeed, only one broad peak is seen in the spectra of SAPO-40 (not shown here) and the two MeAPO-40 phases.

The ^{31}P n.m.r. spectra of the MeAPO-40 samples (*Figure 6*) are intermediate between the spectrum of $AlPO_4$-40 and that of SAPO-40.[2,7] The lines are less well resolved than those observed in the spectrum of $AlPO_4$-

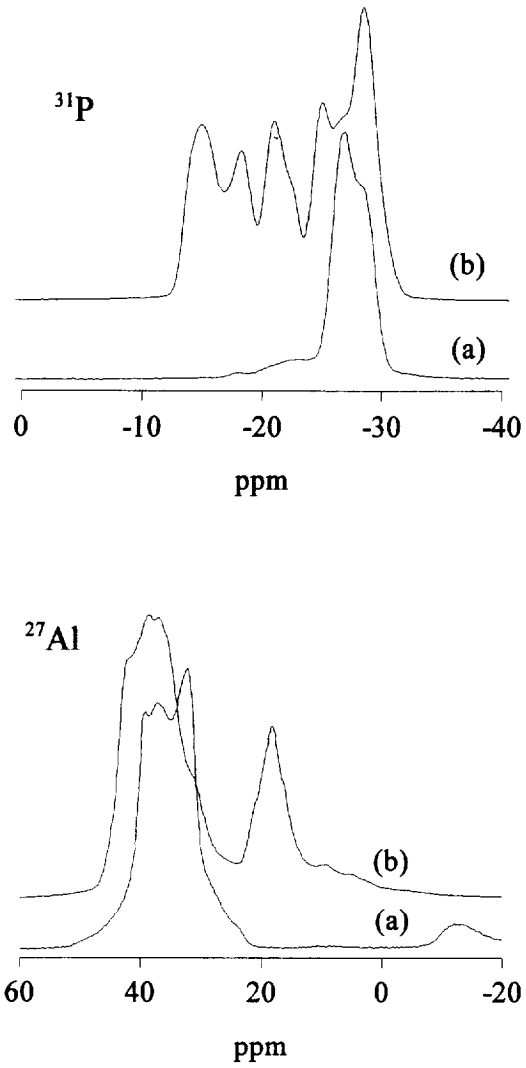

Figure 7 ^{31}P and ^{27}Al *MAS* n.m.r. spectra of as-synthesized (*b*) and calcined (*a*) $AlPO_4$-40.

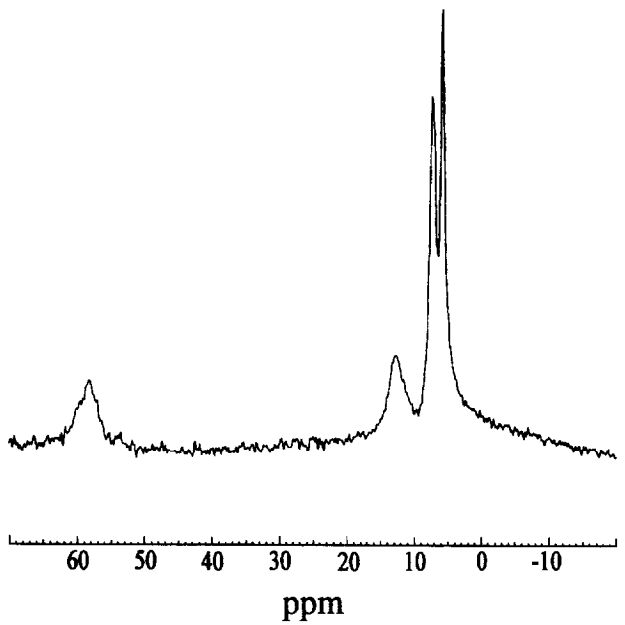

Figure 8 ^{13}C *MAS* n.m.r. spectrum of as-synthesized $AlPO_4$-40.

40, which again accounts for the presence of both nonequivalent T sites (several lines) and the presence of structural defects due to Me insertion (broadening). It should be noted that the presence of paramagnetic Co(II) can influence the profile of the CoAPO-40 n.m.r. spectra.

The ^{27}Al n.m.r. peaks at ca. 18 and 9.8 ppm and the ^{31}P n.m.r. peaks at −15 and −19 ppm have been ascribed, in the case of the SAPO-40,[2,7] to interactions between the concerned T atom (via oxygen) and the template. Indeed, a calcined sample of $AlPO_4$-40 does not show any of these ^{27}Al and ^{31}P n.m.r. resonances when the template is removed upon calcination (*Figure 7*). In the ^{27}Al n.m.r. spectrum, the decomposition of the template also causes a low-frequency shift of all the other lines, but they do not disappear with this treatment (as already reported for SAPO-40[7]). The peak observed at −12 ppm in the ^{27}Al n.m.r. spectrum of the calcined sample is probably due to a residual hydration of the sample.[7] Note that both a structural reorganization upon dehydration at high temperature or the possible presence of some traces of TMA in the structure could also account for the disappearance of the ^{27}Al and ^{31}P n.m.r. peaks. To get more information about the ^{27}Al resonance lines, a detailed study by multiple-quantum ^{27}Al *MAS* n.m.r. spectroscopy is in progress.

Figure 8 shows the ^{13}C n.m.r. spectrum of an as-synthesized $AlPO_4$-40 sample. Although this spectrum was recorded at room temperature, its resolution is similar to that of the ^{13}C n.m.r. spectrum of SAPO-40 recorded at 100°C.[2] This fact suggests that the mobility of the template occluded in the $AlPO_4$-40 structure is larger than in the SAPO-40 structure, probably due to the presence of a noncharged and a nondefected $AlPO_4$-40 framework. The introduction of a heteroelement (Si, Co, Zn, . . .) in the AFR structure generates structural defects, which further reduce the total space available for the template molecules. These molecules will be more tightly confined in a defected structure and thus less mobile. Recent ^{129}Xe n.m.r. evidence confirmed that the internal volume of $AlPO_4$-40 is larger than that of its Co-, Zn-, and Si-substituted counterparts.[23] Furthermore, the spectrum shown in *Figure 8* correlates well with the presence of only tetrapropylammonium ions inside the pore structure, as was found for SAPO-40.[2] It was not possible to obtain clear evidence that traces of tetramethylammonium ions are also occluded in the pore structure, but their presence cannot be definitely excluded.

The ^{13}C n.m.r. results, which indicate that only TPA ions are occluded in the AFR structure, are in agreement with the t.g.a. data (no traces of TMA decomposition were detected) and with the observation that crystals of $AlPO_4$-40 can be formed without the addition of TMA to the synthesis gel. The fact that tetramethylammonium hydroxide helps the crystallization of the AFR structure can be tentatively explained by considering a phenomenon already observed in the case of SAPO-40.[4] In this case, traces of alkali cations (K^+, Na^+) were shown to "quench" the formation of other

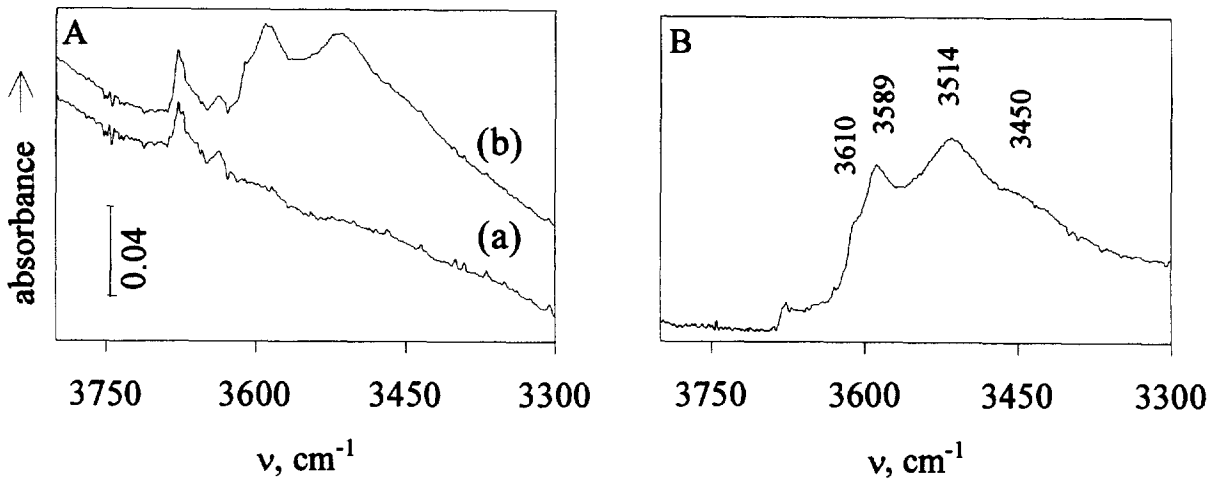

Figure 9 *A*: *FT* i.r. spectra of CoAPO-40: calcined (*a*) and after a hydrogen treatment (*b*). *B*: Difference *FT* i.r. spectrum between CoAPO-40 calcined under oxygen and further reduced under hydrogen.

structures such as AFI that readily appear (more so than AFR) in the absence of these ions. In our case, TMA^+ ions also prevented the formation of AFI in such a way that after a relatively long crystallization time only the AFR structure forms.

FT i.r. spectroscopy

The isomorphous substitution of Al^{3+} for a divalent ion in the tetrahedral positions of an aluminophosphate framework generates a negatively charged lattice. The charges are usually compensated for by the positively charged template ions, which after calcination leave a proton and lead to the formation of Brønsted acid sites. *FT* i.r. spectroscopy is thus a useful tool to study the presence of these OH acid sites and to probe indirectly the framework incorporation of the elements.

As already described, the as-synthesized CoAPO-40 sample is deep blue. After calcination and template removal, the color of the sample changed to yellow-green. We believe that this is due to the oxidation of framework Co^{II} to Co^{III},[19,20,22,24] although certain e.s.r. and t.p.d.-t.g.a. results obtained on CoAPO-5 samples indicate that the color change is due to lattice distortions and not to changes in the Co oxidation state.[25] The cobalt valence state after calcination will be discussed in detail elsewhere.[26,27] However, some features will be mentioned here. The CoAPO-40 sample was calcined under oxygen and then was treated with hydrogen. The bands associated with the OH Brønsted acid sites were only seen by *FT* i.r. after this second treatment (*Figure 9*). The spectrum recorded after the first calcination under oxygen (*Figure 9, curve a*) shows only a band at 3,676 cm^{-1} assigned to P–OH and Al–OH terminal groups. After the hydrogen treatment, two new bands at 3,589 and 3,514 cm^{-1} and two shoulders at 3,610 and 3,450 cm^{-1} appear in the spectrum. We assign these new bands to OH Brønsted acid sites.[26,27] The results found by *FT* i.r. spectroscopy are thus in accord with the hypothesis of a reversible oxidation of the framework cobalt ions, which in turn could cause a possible reversible exclusion/insertion of Co^{III}/Co^{II}, respectively, in the framework positions.

Figure 10 shows the *FT* i.r. spectra of $AlPO_4$-40 and

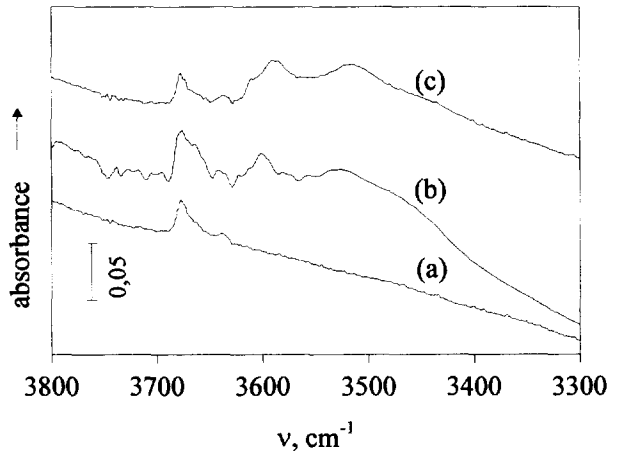

Figure 10 *FT* i.r. spectra of $AlPO_4$-40 (*a*) and ZnAPO-40 (*b*) after an oxidative treatment and CoAPO-40 (*c*) after an oxidative treatment and further reduced under hydrogen.

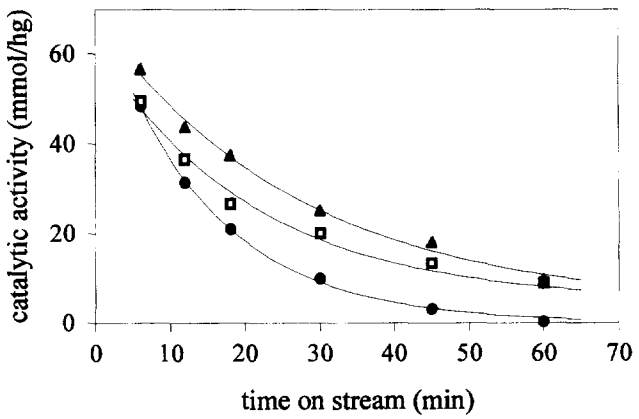

Figure 11 Total catalytic activity of the ZnAPO-40 (▲), CoAPO-40 (●), and SAPO-40 (□) for the *m*-xylene isomerization.

Table 6 Catalytic activity and selectivity parameters calculated at 6 and 30 min on stream

	t = 6 min				t = 30 min				
Sample	*p/o*	I/D	1,3,5 TMB/ ΣTMB	Catal. activity (mmol · h^{-1} · g^{-1})	*p/o*	I/D	1,3,5 TMB/ ΣTMB	Catal. activity (mmol · h^{-1} · g^{-1})	Coke (%)
CoAPO-40	1.14	0.79	0.17	48.4	1.62	0.73	0.10	9.9	2.2
ZnAPO-40	1.06	0.56	0.24	56.6	1.33	0.83	0.16	25.1	2.8
SAPO-40	1.01	0.67	0.26	49.5	1.38	0.72	0.17	20.1	4.1

Note: The coke content was calculated by thermogravimetry after 90 min on stream.

ZnAPO-40 samples after the oxidative calcination and the spectrum of CoAPO-40 after the hydrogen treatment. The *FT* i.r. spectrum of $AlPO_4$-40 only displays a band at 3,676 cm^{-1}, assigned to P–OH and Al–OH terminal groups and in agreement with its neutral framework. Despite the overall low intensity of the bands, the ZnAPO-40 spectrum is similar to that of CoAPO-40. This also indicates the presence OH Brønsted acid sites resulting from the framework incorporation of Zn.

Catalytic tests

The characterization of the CoAPO-40 and ZnAPO-40 samples suggests that cobalt and zinc are incorporated in the AFR framework and, as a consequence, that Brønsted acid sites are generated after the removal of the template. The isomerization of *m*-xylene was used as a model reaction to probe the catalytic activity of the samples and to confirm the presence of the Brønsted acid sites.

As already reported,[26] the pretreatment conditions for CoAPO-40 strongly influence its catalytic activity. *Figure 11* reports the total catalytic activity of CoAPO-40, ZnAPO-40, and, for comparison, SAPO-40 samples. The CoAPO-40 sample was submitted to a treatment under hydrogen flow for 5 h at 500°C after the template removal and before the catalytic testing. The selectivity parameters considered for the analysis of this reaction were the isomerization/disproportionation (I/D), *p*-xylene/*o*-xylene (*p/o*) and 1,3,5-trimethylbenzene/sum of trimethylbenzenes (1,3,5-TMB/ΣTMB) ratios. These and the values of the catalytic activities calculated at 6 and 30 min on stream are collected in *Table 6*. The results of the catalytic activity for the two MeAPO-40 samples, shown in *Figure 11* and *Table 6*, indicate the presence of strong acid sites, confirming the *FT* i.r. data and hence confirming the incorporation of cobalt and zinc into the AFR framework.

The initial catalytic activity shown by the MeAPO-40 samples is similar to that of the SAPO-40 sample tested that has a larger number of acid sites. In addition, SAPO-40 displays a catalytic activity that is similar to that of classical zeolites such as mordenite and ZSM-5.[8] Thus, the results obtained for the MeAPO-40 samples suggest (when compared with SAPO-40) that the acid sites generated by the incorporation of Co and Zn are stronger than those generated by the incorporation of Si. This behavior was previously reported in the case of MeAPSO-34 and SAPO-34 samples.[28]

As already described for SAPO-40,[8] the initial *p/o* and 1,3,5-TMB/ΣTMB ratios, which were close to the values predicted by the thermodynamic equilibrium at 350°C (1.05 and 0.24, respectively) calculated for the two MeAPO-40 samples, are characteristics of an open structure. A small pore blockage is probably the reason for the slightly higher value of the *p/o* ratio and the slightly lower value of the 1,3,5-TMB/TMB ratio. The low value of the isomerization reaction with respect to the disproportionation reaction indicates, for all samples, that the diphenylmethane-type transition state complex of the secondary disproportionation reaction can be accommodated inside the pore structure, thus confirming the presence of a relatively large void volume.[8,29]

In conclusion, the catalytic results show that all the MeAPO-40 samples tested have similar porous structures and contain strong acid sites. These sites appear probably as a result of the framework incorporation of Co and Zn, which generates Brønsted-type sites. The presence of Lewis sites must also be considered.[27]

CONCLUSION

This paper shows the possibility of preparing pure samples of $AlPO_4$-40, CoAPO-40, and ZnAPO-40 in the presence (simultaneously) of both small amounts of tetramethylammonium hydroxide and tetrapropylammonium hydroxide, the usual template agent for the synthesis of SAPO-40. Because $AlPO_4$-40 can also be prepared in the absence of tetramethylammonium hydroxide, and because when introduced in the parent gel tetramethylammonium was never clearly detected in the pore structure, TMA does not seem to play a true templating role in the AFR synthesis. Several characterization techniques indicate that a true framework incorporation of Co and Zn has occurred. The catalytic tests showed that the acid sites generated upon the framework incorporation of Co and Zn are stronger than those resulting from the incorporation of Si in the AFR framework.

ACKNOWLEDGMENTS

Financial support for this work by JNICT, under PRAXIS XXI program and FEDER, is gratefully acknowledged. We also thank IMAT/Aveiro for access to the solid-state n.m.r. and u.v.-vis facilities, S. Valange (Namur) for help in running the EDX experiments, and J.L. Guth (Mulhouse, France) for providing ZnAPO- and CoAPO-type materials with known composition, which were used as standards for EDX measurements.

REFERENCES

1 Lok, B.M., Messina, C.A., Paton, R.L., Gajek, R.T., Cannan, T.R. and Flanigen, E.M. US Pat. 4,440,871 (1984)
2 Dumont, N., Gabelica, Z., Derouane, E.G. and McCusker, L.B. *Microporous Mater.* 1993, **1,** 149
3 Meier, W.M. and Olson, D.H. *Atlas of Zeolite Structure Types,* Butterworth-Heinemann, London, 1992, p. 30
4 Dumont, N., Gabelica, Z., Derouane, E.G. and Di Renzo, F. *Microporous Mater.* 1994, **3,** 71
5 Lourenço, J.P., Ribeiro, M.F., Ribeiro, F.R., Rocha, J., Gabelica, Z., Dumont, N. and Derouane, E.G. *Stud. Surf. Sci. Catal.* 1994, **84,** 867
6 Lourenço, J.P., Ribeiro, M.F., Ribeiro, F.R., Rocha, J. and Gabelica, Z. *J. Chem. Soc. Faraday Trans.* 1995, **91,** 2213
7 Lourenço, J.P., Ribeiro, M.F., Ribeiro, F.R., Rocha, J., Gabelica, Z. and Derouane, E.G. *Microporous Mater.* 1995, **4,** 445
8 Lourenço, J.P., Ribeiro, M.F., Ramôa Ribeiro, F., Rocha, J. and Gabelica, Z. *Appl. Catal. A*
9 Lourenço, J.P., Ribeiro, M.F., Ramôa Ribeiro, F., Rocha, J. and Gabelica, Z. *React. Kinet. Catal. Lett.* 1996, **59,** 219
10 Derewinski, M. and Barthomeuf, D. *Appl. Catal. A* 1995, **128,** 79
11 Sierra, L.S., Patarin, J., Deroche, C., Gies, H. and Guth, J.L. *Stud. Surf. Sci. Catal.* 1994, **84,** 2237
12 Lourenço, J.P., PhD Thesis, Technical University of Lisbon, Lisbon, July 1996
13 Rajic, N., Kaucic, V. and Stojakovic, D. *Zeolites* 1990, **10,** 169
14 Duke, C.V.A., Hill, S.J. and Williams, C.D. *Zeolites* 1995, **15,** 413
15 McCusker, L.B. and Baerlocher, C. *Microporous Mater.* 1996, **6,** 51
16 Roque-Malherbe, R., Lopez-Cordero, R., Gonzalez-Morales, J.A., Oñate-Martinez, J. and Carreras-Gracial, M. *Zeolites* 1993, **13,** 481
17 Elangovan, S.P., Krishnasamy, V. and Murugesan, V. *Catal. Lett.* 1996, **36,** 271
18 Gabelica, Z., B. Nagy, J., Bodart, P., Dewaele, N. and Nastro, A. *Zeolites* 1987, **7,** 67
19 Iton, L.E., Choi, I., Desjardins, J.A. and Maroni, V.A. *Zeolites* 1989, **9,** 535
20 Kraushaar-Czarnetzki, B., Hoogervorst, W.G.M., Andréa, R.R., Emeis, C.A. and Stork, W.H.J. *Stud. Surf. Sci. Catal.* 1991, **69,** 231
21 Singh, P.S., Shaikh, R.A., Bandyopadhyay, R. and Rao, B.S. *J. Chem. Soc., Chem. Commun.* 1995, 2255
22 Marchese, L., Martra, G., Damilano, N., Coluccia, S. and Thomas, J.M. *Stud. Surf. Sci. Catal.* 1996, **101,** 861
23 Gabelica, Z., Ito, T., Lourenço, J.P. and Ribeiro, M.F. Manuscript in preparation
24 Prasad, S. and Balakrishnan, I. *Catal. Lett.* 1991, **11,** 105
25 Kurshev, V., Kevan, L., Parillo, D.J., Pereira, C., Kokotailo, G.T. and Gorte, R.J. *J. Phys. Chem.* 1994, **98,** 10160
26 Lourenço, J.P., Ribeiro, M.F., Ramôa Ribeiro, F., Rocha, J., Gabelica, Z., Onida, B. and Garrone, E. *Stud. Surf. Sci. Catal.* 1997, **105C,** 1973
27 Onida, B., Garrone, E., Lourenço, J.P., Ribeiro, M.F. and Gabelica, Z. Manuscript in preparation
28 Hocevar, S. and Levec, J. *J. Catal.* 1992, **135,** 518
29 Olson, D.H. and Haag, W.O., in *Catalytic Materials: Relationship Between Structure and Reactivity* (Eds. T.E. Whyte et al.) ACS Symp. Ser. 248, Am. Chem. Soc., Washington, DC, 1984, p. 275